Learning Joint Intensity in Multivariate Poisson Processes on Statistical Manifolds

Anonymous Author(s)
Affiliation
Address
email

Abstract

We show that *generalized additive models* (GAMs) can be treated via the *log-linear model* on a structured sample space, which has a well established information geometric background. Connecting GAMs with multivariate stochastic processes, we present the *additive Poisson process* (APP), a novel framework that can model the higher-order interaction effects of the intensity functions in stochastic processes using lower dimensional projections. Learning of the model is achieved via *convex optimization*, thanks to the dually flat statistical manifold generated by the log-linear model.

1 Introduction

Consider two stochastic processes which are correlated with arrival times for an event. For a given time interval, what is the probability of observing an event from both processes? Can we learn the joint intensity function by just using the observations from each individual processes? Our proposed model, the *Additive Poisson Process* (APP), provides a novel solution to this problem.

Our model combines the information geometric techniques introduced by Luo and Sugiyama [2019] to model higher-order interactions between stochastic processes and by Friedman and Stuetzle [1981] in *generalized additive model*s (GAMs) to learn the intensity function using samples in a lower dimensional space. We first show the connection between GAMs and Poisson processes. We then connect GAMs to the *log-linear model* [Agresti, 2012], which has a well-established theoretical background in information geometry [Amari, 2016] and can introduce partial order structures into its sample space [Sugiyama et al., 2017]. The learning process in our model is formulated as a convex optimization problem to arrive at a unique optimal solution using natural gradient, which minimizes the Kullback-Leibler (KL) divergence from the sample distribution in a lower dimensional space to the distribution modeled by the learned intensity function. This connection provides remarkable properties to our model: the ability to learn higher-order intensity functions using lower dimensional projections, thanks to the *Kolmogorov-Arnold representation theorem*. This property makes it advantageous to use our proposed approach for the cases where there are, no observations, missing samples, or low event rate. Our model is flexible because it can capture interaction between processes as a partial order structure in the log-linear model and the parameters of the model is fully customizable to meet the requirements for the application.

2 Formulation

The log-likelihood of the multi-dimensional Poisson process with the functional prior is described as

$$\log p\left(\{\mathbf{t}_i\}_{i=1}^N \mid \lambda\left(\mathbf{t}\right)\right) = \sum_{i=1}^N f\left(\mathbf{t}_i\right) - \int \exp\left(f\left(\mathbf{t}\right)\right) d\mathbf{t}. \tag{1}$$

Submitted to 34th Conference on Neural Information Processing Systems (NeurIPS 2020). Do not distribute.

In the following sections, we introduce *generalized additive models* and propose to model it by the *log-linear model* to learn $f(\mathbf{t})$ and the normalizing term.

2.1 Generalized Additive Model

In this section we present the connection between Poisson processes with Generalized Additive Model (GAM) proposed by Friedman and Stuetzle [1981]. GAM projects higher-dimensional features into lower-dimensional space to apply smoothing functions to build a restricted class of non-parametric regression models. GAM is less affected by the curse of dimensionality compared to directly using smoothing in a higher-dimensional space. For a given set of processes $J \subseteq [D] = \{1, \dots, D\}$, the traditional GAM using one-dimensional projections is defined as $\log \lambda_J(\mathbf{t}) = \sum_{j \in J} f_j(t^{(j)}) - \beta_J$ with some smoothing function f_j.

In this paper, we extend it to include higher-order interactions between features in GAM. The *k-th order GAM* is defined as

$$\begin{aligned}\log \lambda_J(\mathbf{t}) &= \sum_{j \in J} f_{\{j\}}(t^{(j)}) + \sum_{j_1, j_2 \in J} f_{\{j_1, j_2\}}(t^{(j_1)}, t^{(j_2)}) + \cdots + \sum_{j_1, \dots, j_k \in J} f_{\{j_1, \dots, j_k\}}(t^{(j_1)}, \dots, t^{(j_k)}) - \beta_J \\ &= \sum_{I \subseteq J,\, |I| \leq k} f_I(\mathbf{t}^{(I)}) - \beta_J, \end{aligned} \tag{2}$$

where $\mathbf{t}^{(I)} \in \mathbb{R}^{|I|}$ denotes the subvector $(\mathbf{t}^{(j)})_{j \in I}$ of $\mathbf{t}$ with respect to $I \subseteq [D]$. The function $f_I : \mathbb{R}^{|I|} \to \mathbb{R}$ is a smoothing function to fit the data, and the normalization constant β_J for the intensity function is obtained as $\beta_J = \int \lambda_J(\mathbf{t}) d\mathbf{t} = \int \exp(\sum_{I \subseteq J,\, |I| \leq k} f_I(\boldsymbol{t}^{(I)})) d\mathbf{t}$. The definition of the additive model is in the same form as Equation (1). In particular, if we compare Equation (1) and (2), we can see that the smoothing function f in (1) corresponds to the right-hand side of (2).

2.2 Additive Poisson Process

We introduce our key technical contribution in this section, the log-linear formulation of the *additive Poisson process*, and draw parallels between higher-order interactions in the log-linear model and the lower dimensional projections in generalized additive models. In the following, we discretize the time window $[0, T]$ into M bins and treat each bin as a natural number $\tau \in [M] = \{1, 2, \dots, M\}$ for each process. We assume that M is predetermined by the user. First we introduce a structured space for the Poisson process to incorporate interactions between processes. Let $\Omega = \{\, (J, \tau) | J \in 2^{[D]} \setminus \emptyset, \tau \in [M] \,\} \cup \{(\perp, 0)\}$. We define the *partial order* $\preceq$ [Davey and Priestley, 2002] on Ω as

$$(J, \tau) \preceq (J', \tau') \iff J \subseteq J' \text{ and } \tau \leq \tau', \quad \text{for each } \omega = (J, \tau), \omega' = (J', \tau') \in \Omega, \tag{3}$$

and $(\perp, 0) \preceq (J, \tau)$ for all $(J, \tau) \in \Omega$ The relation $J \subseteq J'$ is used to model any-order interactions between stochastic processes [Luo and Sugiyama, 2019] [Amari, 2016, Section 6.8.4] and each τ in (J, τ) represents "time" in our model. Note that the domain of τ can be generalized from $[M]$ to $[M]^D$ to take different time stamps into account, while in the following we assume that observed time stamps are always the same across processes for simplicity. Our experiments in the next section demonstrates that we can still accurately estimate the density of processes. Our model can be applied to not only time-series data but any sequential data.

On any set equipped with a partial order, we can introduce a *log-linear model* [Sugiyama et al., 2016, 2017]. Given a parameter domain $\mathcal{S} \subseteq \Omega$. For a partially ordered set $(\Omega, \preceq)$, the log-linear model with parameters $(\theta_s)_{s \in \mathcal{S}}$ is introduced as

$$p(\omega; \theta) = \frac{1}{\exp \psi(\theta)} \exp\left(\sum\nolimits_{s \in \mathcal{S}} \mathbf{1}_{[s \preceq \omega]} \theta_s\right) \propto \exp\left(\sum\nolimits_{s \in \mathcal{S}} \mathbf{1}_{[s \preceq \omega]} \theta_s\right). \tag{4}$$

for each $\omega \in \Omega$, where $\mathbf{1}_{[\cdot]} = 1$ if the statement in $[\cdot]$ is true and 0 otherwise, and $\psi(\theta) \in \mathbb{R}$ is the partition function uniquely obtained as $\psi(\theta) = \log \sum_{\omega \in \Omega} \exp(\sum_{s \in \mathcal{S}} \mathbf{1}_{[s \preceq \omega]} \theta_s) = -\theta_{(\perp, 0)}$. A special case of this formulation coincides with the density function of the *Boltzmann machines* [Sugiyama et al., 2018, Luo and Sugiyama, 2019]. We have a clear correspondence between the log-linear formulation and that in the form of Kolmogorov-Arnold representation theorem in Equation (8). We call the log-linear model with $(\Omega, \preceq)$ defined in Equation (3) the additive Poisson process, which

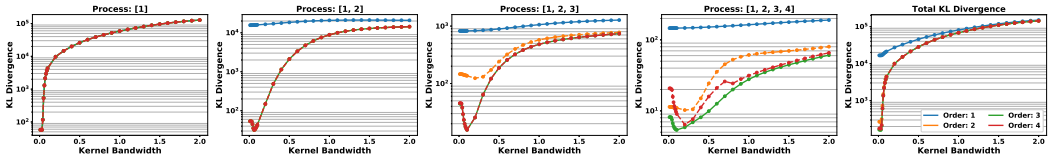

(a) Dense observations.

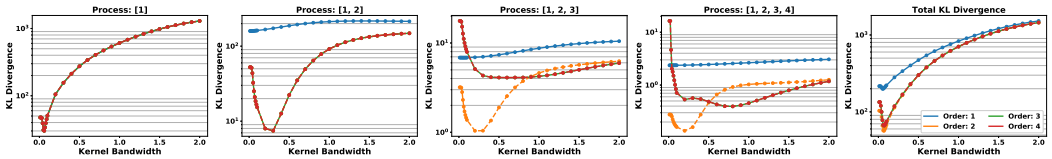

(b) Sparse observations.

Figure 1: KL Divergence for four-order Poisson process.

represents the intensity λ as the joint distribution across all possible states. The intensity λ of the multi-dimensional Poisson process given via the GAM in Equation (8) is fully modeled (parameterized) by Equation (4) and each intensity $f_I(\cdot)$ is obtained as $\theta_{(I,\cdot)}$. To consider the k-th order model, we consistently use the parameter domain $\mathcal{S}$ given as $\mathcal{S} = \{\, (J, \tau) \in \Omega \mid |J| \leq k \,\}$, where k is an input parameter to the model that specifies the upper bound of the order of interactions. This means that $\theta_s = 0$ for all $s \notin \mathcal{S}$. Note that our model is well-defined for any subset $\mathcal{S} \subseteq \Omega$ and the user can use arbitrary domain in applications.

For a given J and each bin τ with $\omega = (J, \tau)$, the empirical probability $\hat{p}(\omega)$, which corresponds to the input observation, is given as

$$\hat{p}(\omega) = \frac{1}{Z} \sum_{I \subseteq J} \sigma_I(\boldsymbol{\tau}), \quad Z = \sum_{\omega \in \Omega} \hat{p}(\omega), \quad \text{and } \sigma_I(\boldsymbol{\tau}) := \frac{1}{N h_I} \sum_{i=1}^{N} K\left(\frac{\boldsymbol{\tau}^{(I)} - \mathbf{t}_i^{(I)}}{h_I} \right) \tag{5}$$

for each discretized state $\omega = (J, \tau)$, where $\boldsymbol{\tau} = (\tau, \ldots, \tau) \in \mathbb{R}^D$. The function σ_I performs smoothing on time stamps $\mathbf{t}_1, \ldots, \mathbf{t}_N$, which is the kernel smoother proposed by Buja et al. [1989]. The function K is a kernel and h_I is the bandwidth for each projection $I \subseteq [D]$. We use the Gaussian kernel as K to ensure that probability is always nonzero, meaning that the definition of the kernel smoother coincides with the kernel estimator of the intensity function proposed by Schäbe [1993].

2.3 Optimization

Given an empirical distribution $\hat{p}$ defined in Equation (5), the task is to learn the parameter $(\theta_s)_{s \in \mathcal{S}}$ such that the distribution via the log-linear model in Equation (4) is close to $\hat{p}$ as much as possible. Let us define $\mathfrak{S}_{\mathcal{S}} = \{p \mid \theta_s = 0 \text{ if } s \notin \mathcal{S}\}$, which is the set of distributions that can be represented by the log-linear model using the parameter domain $\mathcal{S}$. Then the objective function is given as $\min_{p \in \mathfrak{S}_{\mathcal{S}}} D_{\mathrm{KL}}(\hat{p}, p)$, where $D_{\mathrm{KL}}(\hat{p}, p) = \sum_{\omega \in \Omega} \hat{p} \log(\hat{p}/p)$ is the KL divergence from $\hat{p}$ to p. In this optimization, let p^* be the learned distribution from the sample with infinitely large sample size and p be the learned distribution for each sample. Then we can lower bound the uncertainty (variance) $\mathbb{E}[D_{\mathrm{KL}}(p^*, p)]$ by $|\mathcal{S}|/2N$ [Barron and Hengartner, 1998].

Thanks to the well developed theory of *information geometry* [Amari, 2016] for the log-linear model [Amari, 2001], it is known that this problem can be solved by *e-projection*, which coincides with the maximum likelihood estimation, and it is always *convex optimization* [Amari, 2016, Chapter 2.8.3]. The gradient with respect to each parameter θ_s is obtained by $(\partial / \partial \theta_s) D_{\mathrm{KL}}(\hat{p}, p) = \eta_s - \hat{\eta}_s$, where $\eta_s = \sum_{\omega \in \Omega} \mathbf{1}_{[\omega \succeq s]} p(\omega)$. The value η_s is known as the expectation parameter [Sugiyama et al., 2017] and $\hat{\eta}_s$ is obtained by replacing p with $\hat{p}$ in the above equation. If $\hat{\eta}_s = 0$ for some $s \in \mathcal{S}$, we remove s from $\mathcal{S}$ to ensure that the model is well-defined.

Let $\mathcal{S} = \{s_1, \ldots, s_{|\mathcal{S}|}\}$ and $\boldsymbol{\theta} = [\theta_{s_1}, \ldots, \theta_{s_{|\mathcal{S}|}}]^T$, $\boldsymbol{\eta} = [\eta_{s_1}, \ldots, \eta_{s_{|\mathcal{S}|}}]^T$. We can always use the *natural gradient* [Amari, 1998] as the closed form solution of the Fisher information matrix is always available [Sugiyama et al., 2017]. The update step is $\boldsymbol{\theta}_{\text{next}} = \boldsymbol{\theta} - \mathbf{G}^{-1}(\boldsymbol{\eta} - \hat{\boldsymbol{\eta}})$, where the Fisher information matrix $\mathbf{G}$ is obtained as $g_{ij} = \frac{\partial}{\partial \theta_{s_i} \partial \theta_{s_j}} D_{\mathrm{KL}}(\hat{p}, p) = \sum_{\omega \in \Omega} \mathbf{1}_{[\omega \succeq s_i]} \mathbf{1}_{[\omega \succeq s_j]} p(\omega) - \eta_{s_i} \eta_{s_j}$.

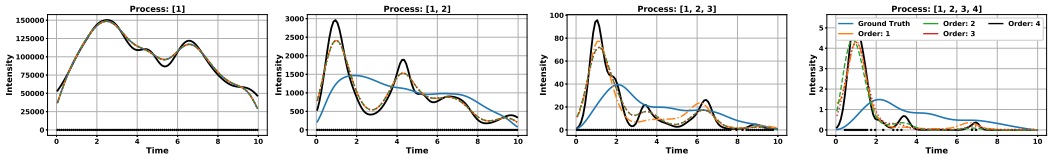

(a) Dense observations.

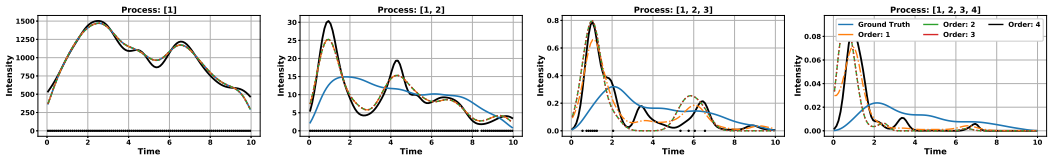

(b) Sparse observations.

Figure 2: Intensity function of higher dimensional processes. Dots represent observations.

3 Experiments

We perform experiments a four dimensional synthetic data to evaluate the performance of our proposed approach. Our code is implemented on Python 3.7.5 with NumPy version 1.8.2 and the experiments are run on Ubuntu 18.04 LTS with an Intel i7-8700 6c/12t with 16GB of memory [1]. In experiments of synthetic data, we simulate random events using Equation (6). We generate an intensity function using a mixture of Gaussians, where the mean is drawn from a uniform distribution and the covariance is drawn from an inverted Wishart distribution. The intensity function is then the density function multiplied by the sample size. The synthetic data is generated by directly drawing a sample from the probability density function with the predetermined sample size. The sample size is randomly chosen by the mixture of Gaussians.

We generate a fourth-order process to simulate the behaviour of the model in higher dimensions. The model is generalizable to higher dimensions, however it is difficult to demonstrate results for processes higher than fourth-order. For our experiment, we generate an intensity function using 50 Gaussian components and draw a sample with the size of 10^7 for the dense case and that with the size of 10^5 for the sparse case. We consider the joint event to be the time frame of 0.1 seconds.

In Figure 1a we observe similar behaviour in the model, where the first-order processes fit precisely to the empirical distribution generated by the Gaussian kernels. The third-order model is able to period better on the fourth-order process. This is because the observation shown in Figure 2a is largely sparse and learning from the observations directly may overfit. A lower dimensional approximation is able to provide a better result in the third-order model. Similar trends can be seen in the sparse case as shown in Figure 1b, where a second-order model is able to produce better estimation in third- and fourth-order processes. The observations are extremely sparse as seen in Figure 2b, where there are only a few observations or no observations at all to learn the intensity function.

4 Conclusion

We have proposed a novel framework, called *Additive Poisson Process* (APP), to learn the intensity function of the higher-order interaction between stochastic processes using samples from lower dimensional projections. We formulated our proposed model using the *the log-linear model* and optimize it using information geometric structure of the distribution space. We drew parallels between our proposed model and *generalized additive model* and showed the ability to learn from lower dimensional projections via the *Kolmogorov-Arnold representation theorem*. Our empirical results have demonstrated the ability to learn higher-order interactions between stochastic processes when there are no or extremely sparse direct observations, and our model is also robust to varying sample sizes. Our approach provides a novel formulation to learn the joint intensity function which typically has extremely low intensity.

[1] The code is available in the supplementary material and will be publicly available online after the peer review process.

References

Alan Agresti. *Categorical Data Analysis*. Wiley, 3 edition, 2012.

S. Amari. Information geometry on hierarchy of probability distributions. *IEEE Transactions on Information Theory*, 47(5):1701–1711, 2001.

Shun-Ichi Amari. Natural gradient works efficiently in learning. *Neural Computation*, 10(2):251–276, 1998.

Sun-Ichi Amari. *Information Geometry and Its Applications*. Springer, 2016.

François Baccelli, Bartłomiej Błaszczyszyn, et al. Stochastic geometry and wireless networks: Volume II applications. *Foundations and Trends in Networking*, 4(1–2):1–312, 2010.

A. Barron and N. Hengartner. Information theory and superefficiency. *The Annals of Statistics*, 26(5): 1800–1825, 1998.

Jürgen Braun. *An application of Kolmogorov's superposition theorem to function reconstruction in higher dimensions*. PhD thesis, Universitäts-und Landesbibliothek Bonn, 2009.

Jürgen Braun and Michael Griebel. On a constructive proof of Kolmogorov's superposition theorem. *Constructive Approximation*, 30(3):653, 2009.

Andreas Buja, Trevor Hastie, and Robert Tibshirani. Linear smoothers and additive models. *The Annals of Statistics*, 17(2):453–510, 1989.

Daryl J Daley and David Vere-Jones. *An Introduction to the Theory of Point Processes: Volume II: General Theory and Structure*. Springer, 2007.

Brian A Davey and Hilary A Priestley. *Introduction to Lattices and Order*. Cambridge University Press, 2002.

Seth Flaxman, Yee Whye Teh, and Dino Sejdinovic. Poisson intensity estimation with reproducing kernels. *Electronic Journal of Statistics*, 11(2):5081–5104, 2017.

Jerome H Friedman and Werner Stuetzle. Projection pursuit regression. *Journal of the American Statistical Association*, 76(376):817–823, 1981.

Deniz Ilalan. A poisson process with random intensity for modeling financial stability. *The Spanish Review of Financial Economics*, 14(2):43–50, 2016.

Andrei Nikolaevich Kolmogorov. On the representation of continuous functions of many variables by superposition of continuous functions of one variable and addition. *Doklady Akademii Nauk*, 114 (5):953–956, 1957.

Athanasios Kottas. Dirichlet process mixtures of beta distributions, with applications to density and intensity estimation. In *Workshop on Learning with Nonparametric Bayesian Methods, 23rd International Conference on Machine Learning (ICML)*, volume 47, 2006.

Simon Luo and Mahito Sugiyama. Bias-variance trade-off in hierarchical probabilistic models using higher-order feature interactions. In *Proceedings of the 33rd AAAI Conference on Artificial Intelligence*, pages 4488–4495, 2019.

Yosihiko Ogata. On Lewis' simulation method for point processes. *IEEE Transactions on Information Theory*, 27(1):23–31, 1981.

Murray Rosenblatt. Remarks on some nonparametric estimates of a density function. *The Annals of Mathematical Statistics*, pages 832–837, 1956.

H Schäbe. Nonparametric estimation of intensities of nonhomogeneous poisson processes. *Statistical Papers*, 34(1):113–131, 1993.

David W Scott. *Multivariate density estimation: theory, practice, and visualization*. John Wiley & Sons, 2015.

Mahito Sugiyama, Hiroyuki Nakahara, and Koji Tsuda. Information decomposition on structured space. In *2016 IEEE International Symposium on Information Theory*, pages 575–579, 2016.

Mahito Sugiyama, Hiroyuki Nakahara, and Koji Tsuda. Tensor balancing on statistical manifold. In *Proceedings of the 34th International Conference on Machine Learning*, volume 70 of *Proceedings of Machine Learning Research*, pages 3270–3279, 2017.

Mahito Sugiyama, Hiroyuki Nakahara, and Koji Tsuda. Legendre decomposition for tensors. In *Advances in Neural Information Processing Systems 31*, pages 8825–8835, 2018.

Matthew A Taddy. Autoregressive mixture models for dynamic spatial poisson processes: Application to tracking intensity of violent crime. *Journal of the American Statistical Association*, 105(492): 1403–1417, 2010.

HR Thompson. Spatial point processes, with applications to ecology. *Biometrika*, 42(1/2):102–115, 1955.

Feng Zhou, Zhidong Li, Xuhui Fan, Yang Wang, Arcot Sowmya, and Fang Chen. A refined MISD algorithm based on Gaussian process regression. In *Pacific-Asia Conference on Knowledge Discovery and Data Mining*, pages 584–596. Springer, 2018.

A Related Work

The Poisson process is a counting process used in a wide range of disciplines such as time-space sequence data including transportation [Zhou et al., 2018], finance [Ilalan, 2016], ecology [Thompson, 1955], and violent crime [Taddy, 2010] to model the arrival times for a single system by learning an intensity function. When the intensity function is multiplied by a time interval, it gives the probability of a point being excited at a given time. Despite the recent advances of modeling of the Poisson processes and its wide applicability, majority of the point processes model only a single stochastic process and do not consider the correlation between two or more stochastic processes. Several models have been proposed to include events from different stochastic processes. Currently, majority of the multivariate Poisson processes found in literature attempt to learn the conditional intensity function. One example of this is the marked Poisson process (MPP) [Baccelli et al., 2010], where the different events are marked so that a particular subset of events can be used to generate the intensity function. Majority of these techniques provide approaches to identify different events to compute the the conditional intensity function. Currently these have been very few attempts to learn of the joint intensity function. Differently, our proposed approach learns the joint intensity function of the stochastic process which is generally more desirable in many applications.

Kernel density estimation (KDE) [Rosenblatt, 1956] can be used to learn the joint intensity function. However, KDE suffers from the curse of dimensionality, which means that KDE requires a large size sample or a high intensity function to build an accurate model. In addition, the complexity of the model expands exponentially with respect to the number of dimensions, which makes it infeasible to compute. Bayesian approaches such as using a mixture of beta distributions with a Dirichlet prior [Kottas, 2006] and Reproducing Kernel Hilbert Space (RKHS) [Flaxman et al., 2017] have been proposed to quantify the uncertainty with a prior for the intensity function. However, these approaches are often non-convex, making it difficult to obtain the global optimal solution. In addition, if observation is sparse, it is hard for these approaches to learn a reasonable intensity function.

All current approaches are unable to efficiently and accurately learn the intensity of the interaction between stochastic processes. This is because the intensity of the joint process is often low, leading to sparse samples or, in an extreme case, no direct observations at all, making it difficult to learn the intensity function from the joint samples. In this paper, we propose a novel framework to learn the higher-order interaction effects of intensity functions in stochastic processes.

B Multivariate Poisson Process

The Poisson process is characterized by an arrival intensity λ:$\mathbb{R}^D \to \mathbb{R}$, where we assume multiple D processes. An inhomogeneous Poisson process is a general type of processes, where the arrival intensity changes with time. The process with time-changing intensity $\lambda(t)$ is defined as a counting process $\mathbb{N}(t)$, which has an independent increment property. For all time $t \geq 0$ and changes in time $\delta \geq 0$, the probability p for the observations is given as $p(\mathbb{N}(t+\delta) - \mathbb{N}(t) = 0) = 1 - \delta\lambda(t) + o(\delta)$, $p(\mathbb{N}(t+\delta) - \mathbb{N}(t) = 1) = \delta\lambda(t) + o(\delta)$, and $p(\mathbb{N}(t+\delta) - \mathbb{N}(t) \geq 2) = o(\delta)$, where $o(\cdot)$ denotes little-o notation [Daley and Vere-Jones, 2007]. Given a realization of timestamps $\mathbf{t}_1, \mathbf{t}_2, \ldots, \mathbf{t}_N$ with $\mathbf{t}_i \in [0, T]^D$ from an inhomogeneous (multi-dimensional) Poisson process with the intensity λ. Each $\mathbf{t}_i$ is the time of occurrence for the i-th event across D processes and T is the observation duration. The likelihood for the Poisson process [Daley and Vere-Jones, 2007] is given by

$$p\left(\{\mathbf{t}_i\}_{i=1}^N \mid \lambda\left(\mathbf{t}\right)\right) = \exp\left(-\int \lambda\left(\mathbf{t}\right) d\mathbf{t}\right) \prod_{i=1}^N \lambda\left(\mathbf{t}_i\right), \tag{6}$$

where $\mathbf{t} = [t^{(1)}, \ldots, t^{(D)}] \in \mathbb{R}^D$. We define the functional prior on $\lambda(\mathbf{t})$ as

$$\lambda(\mathbf{t}) := g\left(f(\mathbf{t})\right) = \exp\left(f(\mathbf{t})\right). \tag{7}$$

The function $g(\cdot)$ is a positive function to guarantee the non-negativity of the intensity which we choose to be the exponential function, and our objective is to learn the function $f(\cdot)$.

C Kolmogorov-Arnold Representation Theorem

Learning of a continuous function using lower dimensional projections is well known because of the *Kolmogorov-Arnold representation theorem*, which states as follows:

Theorem 1 (Kolmogorov–Arnold Representation Theorem [Braun and Griebel, 2009, Kolmogorov, 1957])**.** *Any multivariate continuous function can be represented as a superposition of one–dimensional functions, i.e.,* $f\left(t_1, \ldots, t_n\right) = \sum_{q=1}^{2n+1} f_q\left(\sum_{p=1}^{n} g_{q,p}\left(t_p\right)\right)$.

Braun [2009] showed that the GAM is an approximation to the general form presented in Kolmogorov-Arnold representation theorem by replacing the range $q \in \{1, \ldots, 2n+1\}$ with $I \subseteq J$ and the inner function $f_{q,p}$ by the identity if $q = p$ and zero otherwise, yielding $f(\mathbf{t}) = \sum_{I \subseteq J} f_I(\mathbf{t}^{(I)})$.

Interestingly, the canonical form for additive models in Equation (2) can be rearranged to be in the same form as Kolmogorov-Arnold representation theorem. By letting $f(\mathbf{t}) = \sum_{I \subseteq J} f_I(\mathbf{t}^{(I)}) = g^{-1}(\lambda(\mathbf{t}))$ and $g(\cdot) = \exp(\cdot)$, we have

$$\lambda_J(\mathbf{t}) = \frac{1}{\exp\left(\beta_J\right)} \exp\left(\sum\nolimits_{I \subseteq J} f_I\left(\mathbf{t}^{(I)}\right)\right) \propto \exp\left(\sum\nolimits_{I \subseteq J} f_I\left(\mathbf{t}^{(I)}\right)\right), \tag{8}$$

where we assume $f_I(\mathbf{t}^{(I)}) = 0$ if $|I| > k$ for the k-th order model and $1/\exp(\beta_J)$ is the normalization term for the intensity function. Based on the Kolmogorov-Arnold representation theorem, generalized additive models are able to learn the intensity of the higher-order interaction between stochastic processes by using projections into lower dimensional space.

D Additional Experiments

Our code is implemented on Python 3.7.5 with NumPy version 1.8.2 and the experiments are run on Ubuntu 18.04 LTS with an Intel i7-8700 6c/12t with 16GB of memory [2]. In experiments of synthetic data, we simulate random events using Equation (6). We generate an intensity function using a mixture of Gaussians, where the mean is drawn from a uniform distribution and the covariance is drawn from an inverted Wishart distribution. The intensity function is then the density function multiplied by the sample size. The synthetic data is generated by directly drawing a sample from the probability density function with the predetermined sample size. The sample size is randomly chosen by the mixture of Gaussians. We then run our models and compare with Kernel Density Estimation (KDE) [Rosenblatt, 1956], an inhomogeneous Poisson process whose intensity is estimated by a reproducing kernel Hilbert space formulation (RKHS) [Flaxman et al., 2017], and a Dirichlet process mixture of Beta distributions (DP-beta) [Kottas, 2006]. The hyper-parameters M and h in our proposed model are selected using grid search and cross-validation. For situations where a validation set is not available, then h could be selected using a rule of thumb approach such as Scott's Rule [Scott, 2015] and M could be selected empirically from the input data by computing the time interval of the joint observation.

D.1 Bandwidth Sensitivity Analysis

Our first experiment is to demonstrate the ability for our proposed model to learn an intensity function from samples. We generate a Bernoulli process with probably of $p = 0.1$ to generate samples for every 1 seconds for 100 seconds to create a toy problem for our model. This experiment is to observe the behaviour of varying the bandwidth in our model. In Figure 3a, we observe that applying no kernel, we learn the deltas of each individual observation. When we apply a Gaussian kernel, the

[2] The code is available in the supplementary material and will be publicly available online after the peer review process.

(a) The lowest KL divergence from the ground truth distribution to the obtained distribution on two types of single processes ([1] and [2]) and joint process of them ([1,2]). APP-# represents the order of the Additive Poisson Process. Missing values mean that the computation did not finish within two days.

	Process	APP-1	APP-2	KDE	RKHS	DP-beta
Dense	[1]	**4.98e-5**	**4.98e-5**	2.81e-4	-	-
	[2]	**2.83e-5**	**2.83e-5**	1.17e-4	-	-
	[1,2]	2.98e-2	1.27e-3	**6.33e-4**	4.09e-2	4.54e-2
Sparse	[1]	**7.26e-4**	**7.26e-4**	8.83e-4	1.96e-2	2.62e-3
	[2]	**2.28e-4**	**2.28e-4**	2.76e-4	2.35e-3	2.49e-3
	[1,2]	2.88e-2	1.77e-2	**3.67e-3**	1.84e-2	3.68e-2

(b) Negative test log-likelihood for the New York Taxi data. Single processes ([T] and [W]) and joint process of them ([T,W]). APP-# represents the order of the Additive Poisson Process.

	Process	APP-1	APP-2	KDE	RKHS	DP-beta
Jan	[T]	714.07	714.07	**713.77**	728.13	731.01
	[W]	745.60	745.60	**745.23**	853.42	790.04
	[T,W]	249.60	**246.05**	380.22	259.29	260.30
Feb	[T]	**713.43**	**713.43**	755.71	908.52	765.76
	[W]	**738.66**	**738.66**	773.65	1031.00	792.10
	[T,W]	328.84	**244.21**	307.86	348.96	326.52
Mar	[T]	**716.72**	**716.72**	733.74	755.48	741.28
	[W]	**738.06**	**738.06**	816.99	853.33	832.43
	[T,W]	291.20	**246.19**	289.69	328.47	300.36

output of the model for the intensity function is much more smooth. Increasing the bandwidth of the kernel will provide a wider and much smoother function. Between the 60 seconds and 80 seconds mark, it can be seen when two observations have overlapping kernels, the intensity function becomes larger in magnitude.

D.2 One Dimensional Poisson Process

A one dimensional experiment is simulated using Ogata's thinning algorithm [Ogata, 1981]. We generate two experiments use the standard sinusoidal benchmark intensity function with a frequency of 20π. The dense experiment has troughs with 0 intensity and peaks at 201 and the sparse experiment has troughs with 0 intensity and peaks at 2. Figure 3d shows the experimental results of the dense case, our model has no problem learning the intensity function. We compare our results using KL divergence between the underlying intensity function used to generate the samples to the intensity function generated by the model. Figure 3b shows that the optimal bandwidth is $h = 1$.

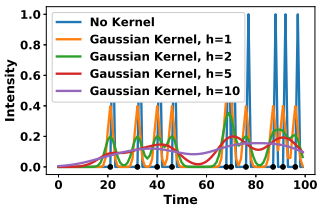

(a) Toy Example

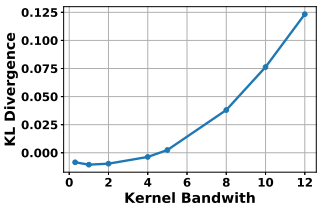

(b) KL divergence of dense experiment

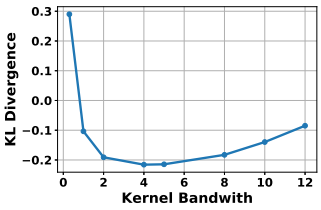

(c) KL divergence of sparse experiment

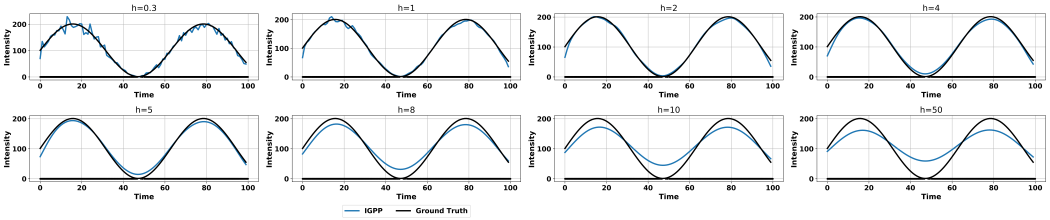

(d) Ogata's thinning algorithm with high intensity

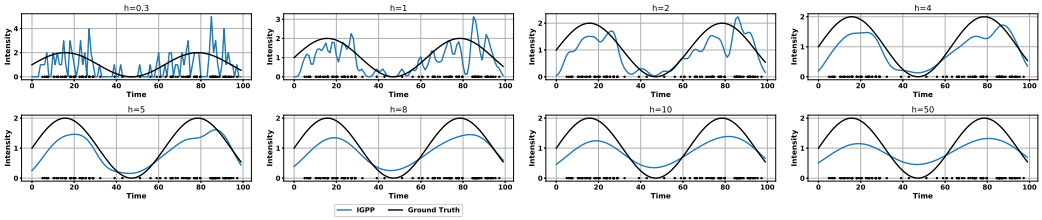

(e) Ogata's thinning algorithm with low intensity

Figure 3: One dimensional experiments

Algorithm 1 Thinning Algorithm for non-homogenous Poisson Process

Function Thinning Algorithm $(\lambda(t), T)$:
$n = m = 0$, $t_0 = s_0 = 0$, $\bar{\lambda} = \sup_{0 \le t \le T} \lambda(t)$
repeat
  $u \sim \text{uniform}(0, 1)$
  $w = -\frac{1}{\bar{\lambda}} \ln u \; \{w \sim \text{exponential}(\bar{\lambda})\}$
  $s_{m+1} = s_m + w$
  $D \sim \text{uniform}(0, 1)$
  if $D \le \frac{\lambda(s_{m+1})}{\bar{\lambda}}$ **then**
    $t_{n+1} = s_{m+1}$
    $n = n + 1$
  else
    $m = m + 1$
  end if
  if $t_n \le T$ **then**
    return $\{t_k\}_{k=1,2,\ldots,n}$
  else
    return $\{t_k\}_{k=1,2,\ldots,n-1}$
  end if
until $s_m \le T$
End Function

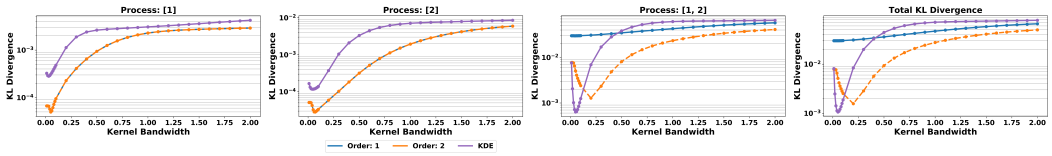

(a) Dense observations.

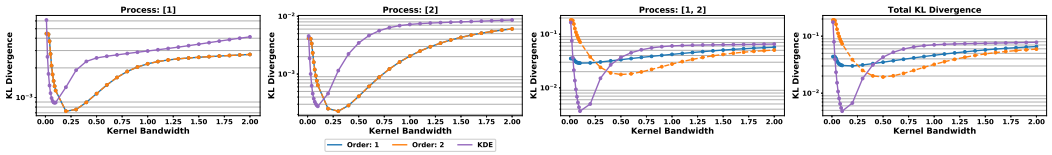

(b) Sparse observations.

Figure 4: KL Divergence for four-order Poisson process.

(a) Dense observations, $h = 0.4$.

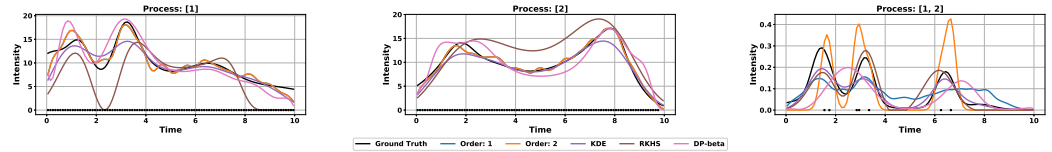

(b) Sparse observations, $h = 0.2$.

Figure 5: Intensity function of two dimensional processes. Dots represent observations.

D.3 Experiments on Two-Dimensional Processes

For our experiment, we use 20 Gaussian components and simulate a dense case with 100,000 observations and a sparse case with 1,000 observations within the time frame of 10 seconds. We consider that a joint event occurs if the two events occur 0.1 seconds apart. Figure 4a and Figure 4b compares the KL divergence between the first- and second-order models. In the first-order processes, both first- and second-order models have the same performance. This is expected as both of the model can treat first-order interactions and is able to learn the empirical intensity function exactly which is the superposition of the one-dimensional projection of the Gaussian kernels on each observation. For the second-order process, the second-order model performs better than the first-order model because it is able to directly learn the intensity function from the projection onto the two-dimensional space. In contrast, the first-order model must approximate the second-order process using the observations from the first order-processes. In the sparse case, the second-order model performs better when the correct bandwidth is selected.

Table 1a compares our approach APP with other state-of-the-art approaches. APP performs the best for first-order processes in both the sparse and dense experiments. Experiments for RKHS and DP-beta were unable to complete running within 2 days for the dense experiment. In the second-order process our approach was outperformed by KDE, while both the second-order APP is able to outperform both RKHS and DP-beta process for both sparse and dense experiments. Figure 4a and Figure 4b show that KDE is sensitive to changes in bandwidth, which means that, for any practical implementation of the model, second-order APP with a less sensitive bandwidth is more likely to learn a more accurate intensity function when the ground truth is unknown.

D.4 Uncovering Common Patterns in the New York Taxi Dataset

We demonstrate the capability of our model on the 2016 Green Taxi Trip dataset[3]. We are interested in finding the common pick up patterns across Tuesday and Wednesday. We define a common pick up time to be within 1 minute intervals of each other between the two days. We have chosen to learn an intensity function using the Poisson process for Tuesday and Wednesday and a joint process for both of them. The joint process uncovers the common pick up patterns between the two days. We have selected to use the first two weeks of Tuesday and Wednesday in January 2016 as our training and validation sets and Tuesday and Wednesday of the third week of January 2016 as our testing set. We repeat the same experiment for February and March.

We show our results in Table 1b, where we use the negative test log-likelihood as an evaluation measure. APP-2 has consistently outperformed all the other approaches for the joint process between Tuesday and Wednesday. In addition, for the individual process, APP-1 and -2 also showed the best result for February and March. These results demonstrate the effectiveness of our model in capturing higher-order interactions between processes, which is difficult for the other existing approaches.

[3] https://data.cityofnewyork.us/Transportation/2016-Green-Taxi-Trip-Data/hvrh-b6nb

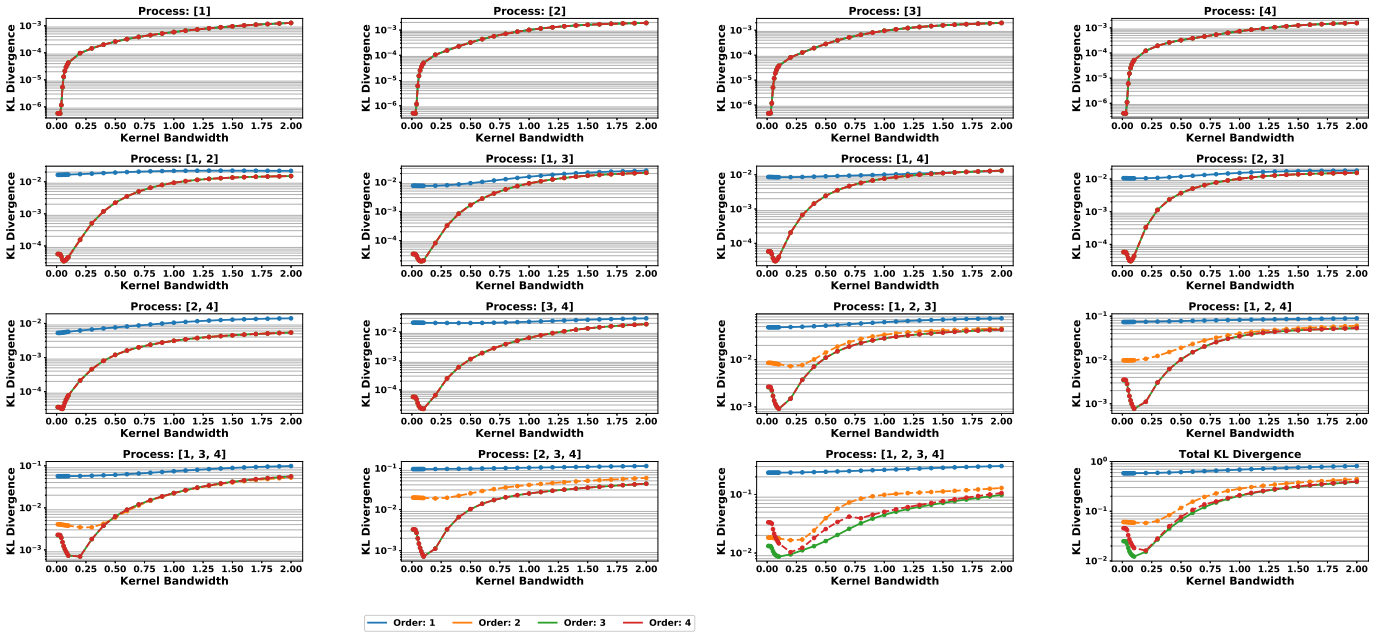

(a) Dense observations.

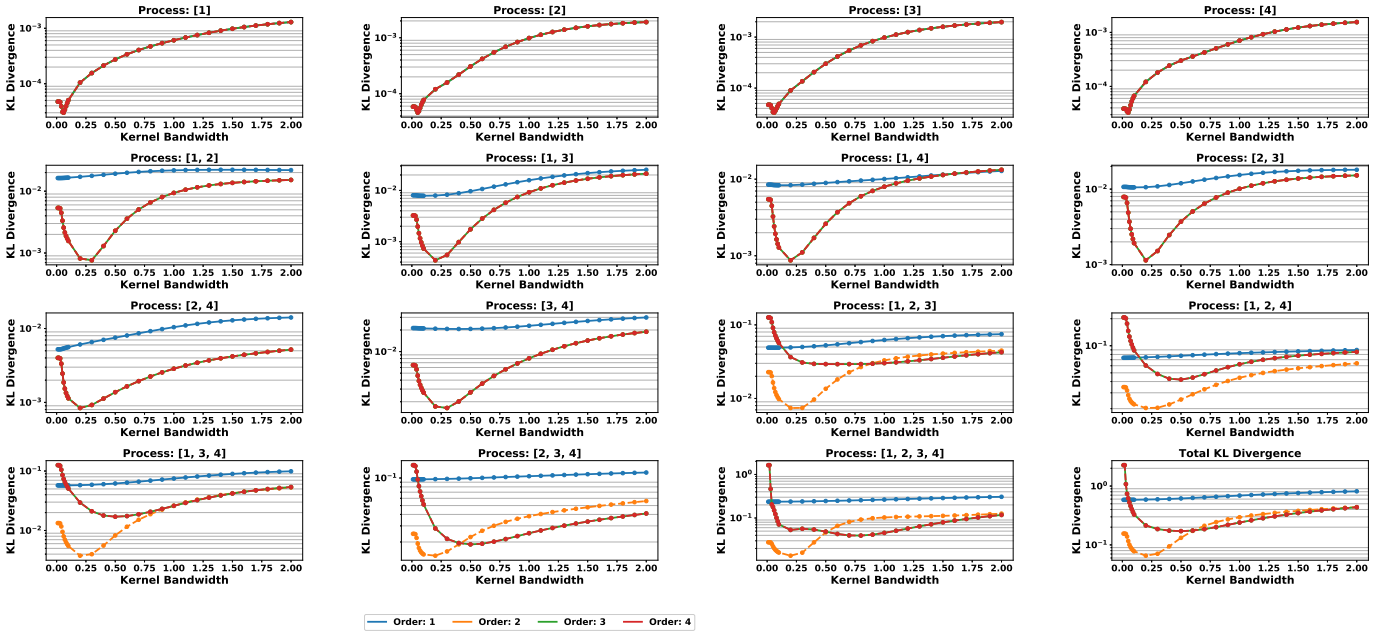

(b) Sparse observations.

Figure 6: KL Divergence for four-order Poisson process.

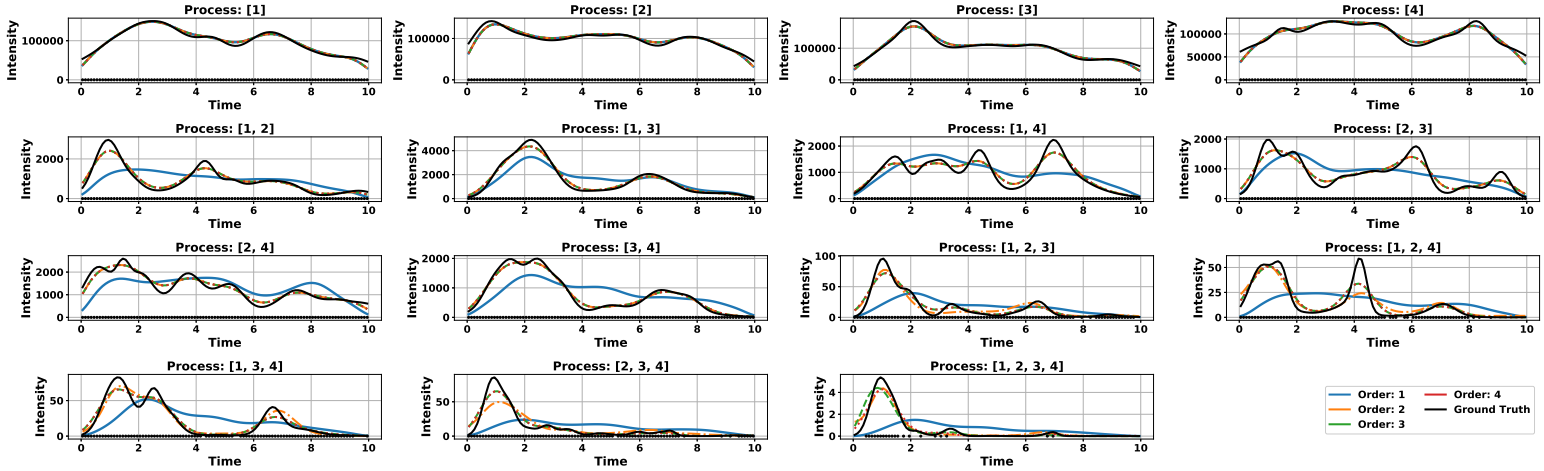

(a) Dense observations.

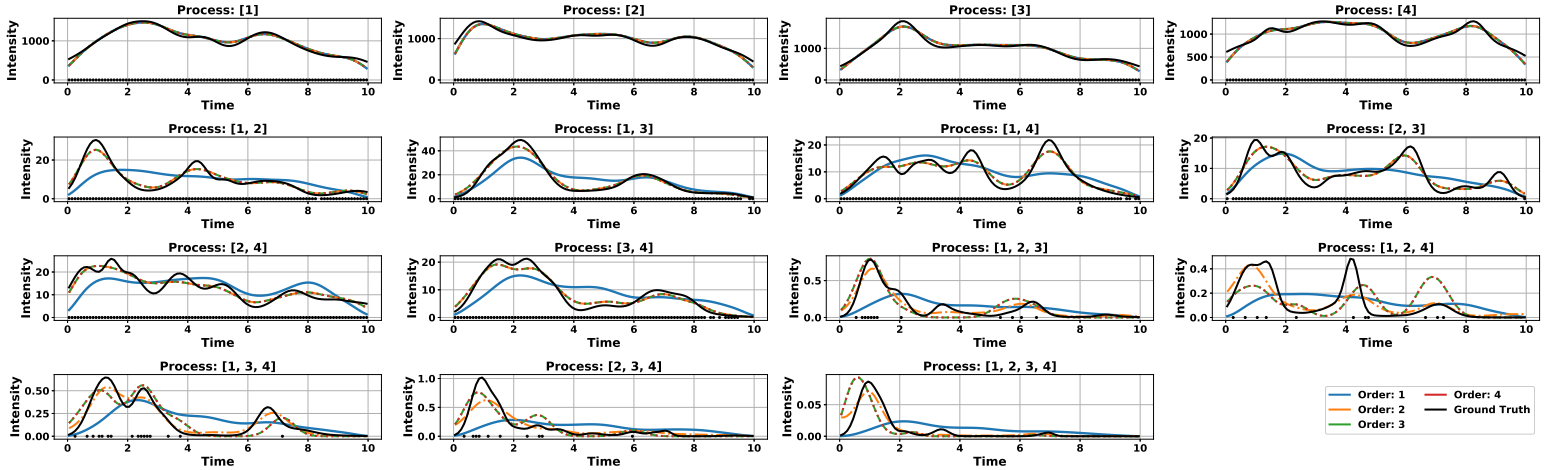

(b) Sparse observations.

Figure 7: Intensity function of higher dimensional processes. Dots represent observations.